Available online at www.sciencedirect.com
ScienceDirect
Journal of the European Ceramic Society 29 (2009) 187–194
www.elsevier.com/locate/jeurceramsoc

Reaction synthesis of layered ternary Ti_2AlC ceramic

V. Gauthier-Brunet *, T. Cabioc'h, P. Chartier, M. Jaouen, S. Dubois

Laboratoire de Physique des Matériaux (UMR 6630 CNRS), Bât. SP2MI, Bd M. & P. Curie, BP 30179, 86962 Futuroscope-Chasseneuil du Poitou, France

Received 23 January 2008; received in revised form 14 May 2008; accepted 24 May 2008
Available online 17 July 2008

Abstract

Reactive sintering of 8Ti:Al_4C_3:C powder mixtures to form the ternary carbide Ti_2AlC is studied in the temperature range 570–1400 °C. After sintering at 1400 °C for 1 h, only the MAX phase Ti_2AlC and some TiC are produced. A series of intermediate phases, such as TiC, Ti_3Al, Ti_3AlC are detected during the reactive sintering process. From X-ray diffraction (XRD) and scanning electron microscopy (SEM) characterizations, a reaction path is proposed for the intermediate phases and Ti_2AlC formation. Results show that reaction kinetics may play an important role in the understanding of the reaction mechanisms.

Keywords: Sintering; Carbides; Microstructure; Electron microscopy; Ti_2AlC

1. Introduction

Ti_2AlC belongs to a class of ternary ceramics generally called MAX phases; this last denomination coming from their general formula $M_{n+1}AX_n$ ($n = 1$–3), where M is a transition metal, A is an A-group element, and X is either C or N.[1–3] The crystal structure of these so-called MAX phases can be described as a stacking of near-close-packed transition metal carbide/nitride layers interleaved with layers of pure A-group elements. In the M_2AX phases, every third layer is an A-group element layer.[1] These ceramics have attracted growing interest and have promoted extensive research activity. Indeed, the metallic nature of the Ti–Ti bonding and the nano-layered nature of the Ti_2AlC structure give rise to a unique combination of metallic and ceramic properties.[4–7] For example, Ti_2AlC has been reported to have excellent machinability at room temperature, high electrical conductivity, high yield strength, and significant plasticity at high temperatures.[8,9]

In the early 1960s, Ti_2AlC was first synthesized by Jeitschko et al.[1] by annealing elemental powders in evacuated quartz tubes for 150 h at 1000 °C. In the mid 1970s, Ivchenko et al. fabricated 90–92% dense Ti_2AlC and measured some of its properties.[10] In that work, Ti_2AlC was prepared by direct synthesis from Al, Ti and lamp black powders at 900–1000 °C for 1 h under argon. The resultant products were then ground to powders and sintered in vacuum at 1500 °C. In 1997 and 2000, Barsoum and El-Raghy reported on the synthesis of fully dense bulk polycrystalline samples of pure Ti_2AlC fabricated from Ti, Al_4C_3 and C powder blends by reactive hot pressing (HP) at 1600 °C for 4 h under a pressure of 40 MPa,[8] and reactive hot isostatic pressing (HIP) at 1300 °C, 40 MPa, 30 h.[9] In 2003, Hong et al. reported for the first time on the synthesis of dense bulk single-phase Ti_2AlC material by the spark plasma sintering (SPS) technology using Ti, Al, and active carbon elemental powders treated at 1100 °C, a temperature lower than that of HP and HIP processes.[11] Recently, to limit the long processing time and to eliminate the need for high-temperature furnaces used in conventional material fabrication, Ti_2AlC was synthesized from Ti, Al and C powder blends by combustion synthesis.[12,13] In addition to the ternary carbide, an appreciable amount of TiC was formed using this far from equilibrium method. Employing thermal explosion mode,[12] Khoptiar and Gotman have shown that combustion synthesis of Ti_2AlC proceeds in three stages: (1) combustion synthesis reaction between Ti and Al with the formation of titanium aluminides; (2) combustion synthesis reaction between Ti and C with the formation of the sub-stoichiometric TiC_x; (3) peritectic reaction between solid $TiC_{0.6–0.7}$ and liquid titanium aluminides with the formation of Ti_2AlC during cooling from the combustion temperature. According to Liu et al.,[13] the ternary Ti_2AlC carbide is formed through a dissolution–precipitation mechanism, in which the formerly produced TiC particles dissolve into the Ti–Al melt and then Ti_2AlC is precipitated as final

* Corresponding author. Tel.: +33 5 49 49 67 52; fax: +33 5 49 49 66 92.
E-mail address: veronique.gauthier@univ-poitiers.fr (V. Gauthier-Brunet).

0955-2219/$ – see front matter © 2008 Elsevier Ltd. All rights reserved.
doi:10.1016/j.jeurceramsoc.2008.05.039

product. However, studies of the reaction mechanisms should be extended to the promising Ti, Al_4C_3 and C powder mixtures[8,9] in order to identify the intermediate phases and to propose a mechanism for the formation of pure Ti_2AlC.

In this paper, we report on the synthesis of Ti_2AlC by reactive sintering starting with Ti, Al_4C_3 and graphite powders. The main purpose of this work is to study the reaction mechanisms operating during the formation of Ti_2AlC using X-ray diffraction (XRD), scanning electron microscopy (SEM) and energy dispersive spectroscopy (EDS).

2. Experimental details

Powders of Ti (Alfa Aesar, 99.5% purity, 100–300 μm), Al_4C_3 (Sigma–Aldrich, 5–20 μm), and C (Alfa Aesar, graphite, 5–10 μm) were used as starting materials. The Ti:C:Al_4C_3 ratio was 8:1:1 (at.%). It is important to immediately note that SEM observations reveal the presence of some Al_2O_3 grains on the surface of the initial Al_4C_3 particles. After sintering, a small amount of Al_2O_3 is still observed. Because of its high stability, one can assume that the Al_2O_3 phase is not involved in the reaction mechanisms responsible for the formation of Ti_2AlC. For such a reason, the presence of Al_2O_3 grains will not be further discussed.

To prepare homogeneous mixtures corresponding to the desired stoichiometry, powders were milled for 1 h in enclosed air with a vibratory ball-mill SPEX 8000 using stainless steel container and balls, and a ball-to-powder mass ratio of 8:1. The different mixtures were cold-compacted into cylindrical steel dies using a uniaxial pressure of 800 MPa. The green density, evaluated from weight and geometric measurements, ranged from 77 to 81% of the theoretical density.

Sintering of the compacts was carried out in a high sensitivity (±0.5 μm) dilatometric system (Setaram Setsys 16/18) under high purity argon. The compacts were sintered at different temperatures, in the range 570–1400 °C, for 1 h under high purity argon. Heating and cooling were performed at an identical temperature rate of 10 °C min^{-1}.

Phase identification was determined by XRD analyses using a Bruker D501 diffractometer with Cu Kα radiation. Microstructures were examined by SEM (JEOL 5600LV) coupled with EDS (Oxford Isis 300) for chemical analysis.

3. Results

3.1. Reactant characteristics

In order to avoid mechanical alloying of Ti and C powders and the resulting formation of TiC during milling operation, the milling time was short and limited to 1 h for the (8Ti + C + Al_4C_3) reactant mixtures. Indeed, no peaks other than those of the Ti and Al_4C_3 starting elements are observed in the XRD pattern of these vibratory milled blends. Diffraction peaks from graphite are no more visible; such a result being simply attributed to the carbon particles amorphization during the milling process.[14] A representative back-scattered SEM image performed on the cross-section of mechanically activated

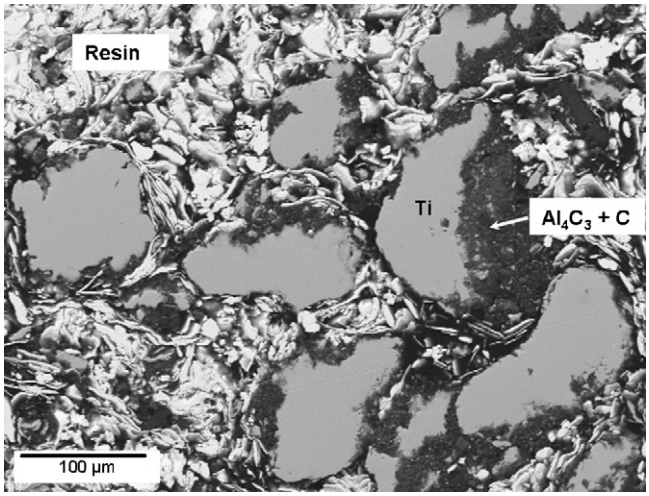

Fig. 1. Back-scattered SEM micrograph of the cross-section of (8Ti + Al_4C_3 + C) powders co-milled for 1 h in the vibratory ball-mill SPEX8000.

powders (embedded in a conductive resin) is shown in Fig. 1. Corresponding EDS analyses demonstrate that the powder reactants consist in 50–200 μm Ti particles embedded in a darker coating constituted of Al_4C_3 and C particles.

3.2. Study of the structural and morphological evolution during the formation of Ti_2AlC by reactive sintering

The thermal expansion curve of a cold-compacted 8Ti:Al_4C_3:C sample heated at 1400 °C for 1 h is shown in Fig. 2. At 570, 800 and 1200 °C, slope variations of the thermal expansion curve are characteristic of a dimensional change of the sample. Thus, for each characteristic temperature (i.e. 570, 800 and 1200 °C) and for the intermediate temperatures (i.e. 900, 1000, 1100, 1200, 1300, 1400 °C) in the thermal expansion curves, a 1-h sintering treatment has been performed under argon. Corresponding XRD and SEM/EDS analyses have been carried out, to identify and to localize the intermediate phases, in order to propose a reaction mechanism for the formation of Ti_2AlC.

XRD patterns related to the samples sintered for 1 h in the temperature range 570–1400 °C have been recorded in the 2θ range 5–100°. For the sake of clarity, Fig. 3 only shows the XRD

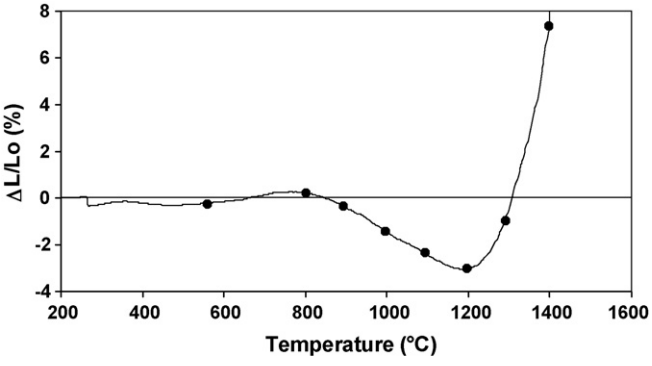

Fig. 2. Thermal expansion curve of cold-compacted 8Ti:Al_4C_3:C reactant mixtures heated at 1400 °C for 1 h.

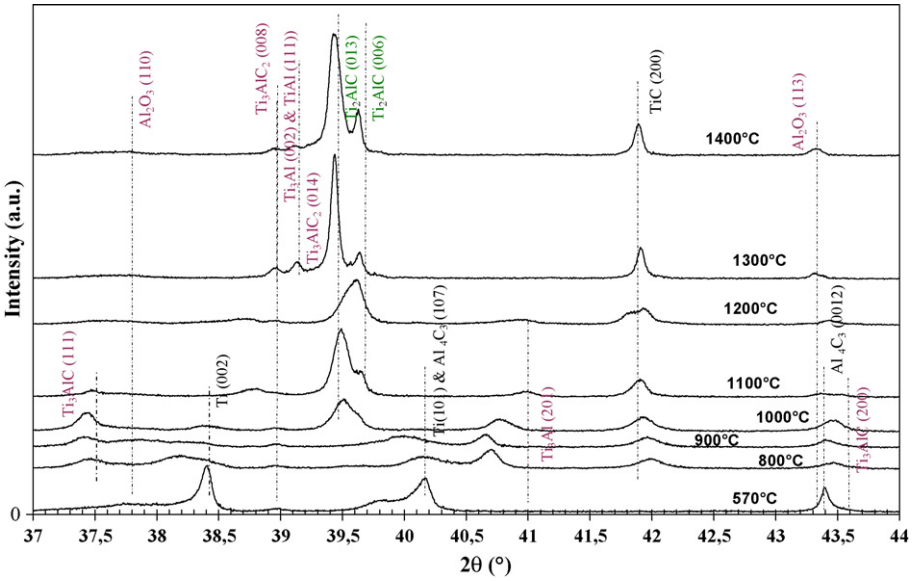

Fig. 3. X-ray diffraction patterns of the co-milled ($8Ti + Al_4C_3 + C$) powder mixtures sintered at different temperatures for 1 h.

patterns in the 2θ range 37–44°. In this figure, the theoretical position of the various (hkl) peaks related to the different phases is pointed out using dotted lines. These XRD patterns have been recorded in the same experimental conditions. As a result, the analysed volume is the same whatever the sintering temperature is. Therefore, as illustrated in Fig. 4, a rough estimation of the evolution of the various phases contents can be deduced from the areas of the main diffraction peaks by assuming that sintered products do not present any texture. A qualitative discussion of the formation and disappearance of the different phases can thus be carried out from the XRD results. A Rietveld analysis was not systematically performed because of the numerous intermediate phases operating during Ti_2AlC formation.

For the first sample sintered at 570 °C, diffraction peaks from unreacted Ti and Al_4C_3 are observed. A more detailed analysis of the XRD pattern gives evidence of a shoulder in the (0 0 2) and (1 0 1)Ti peaks at low angles. As it will be discussed later, the presence of such a contribution at higher lattice spacing may result from the insertion of Al atoms into Ti crystals. A diffraction peak at $2\theta = 38.9°$, which may be attributed to (1 1 1)TiAl, is also detected. Moreover, one can observe the presence of a large peak at $2\theta = 37.8°$ resulting from the presence of small Al_2O_3 grains (which presence was already detected in the initial Al_4C_3 powder). Furthermore, we can immediately note that TiAl and Al_2O_3 peaks are visible over the whole temperature range investigated in this study. After sintering at 800 °C, diffraction peaks from Ti_3Al, Ti_3AlC, and sub-stoichiometric $TiC_{x'}$ are observed in addition to those previously detected at 570 °C. The amount of Ti and Al_4C_3 phases decreases significantly from 570 to 1000 °C, and it is reduced to zero at 1100 °C. After sintering at 900 °C and for higher temperatures, the Ti_3Al content decreases while the Ti_3AlC content increases significantly in the temperature range 900–1000 °C. The detailed analysis of the XRD spectra obtained in the temperature range 800–1000 °C gives evidence for an offset of the (2 0 1)Ti_3Al peak towards lower angles compared to the stoichiometric one. Such an off-

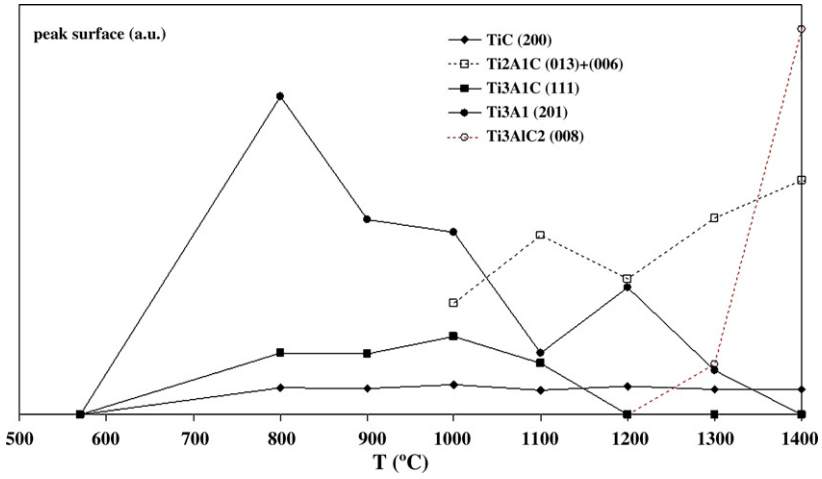

Fig. 4. XRD peak areas of the different phases calculated as a function of the sintering temperature.

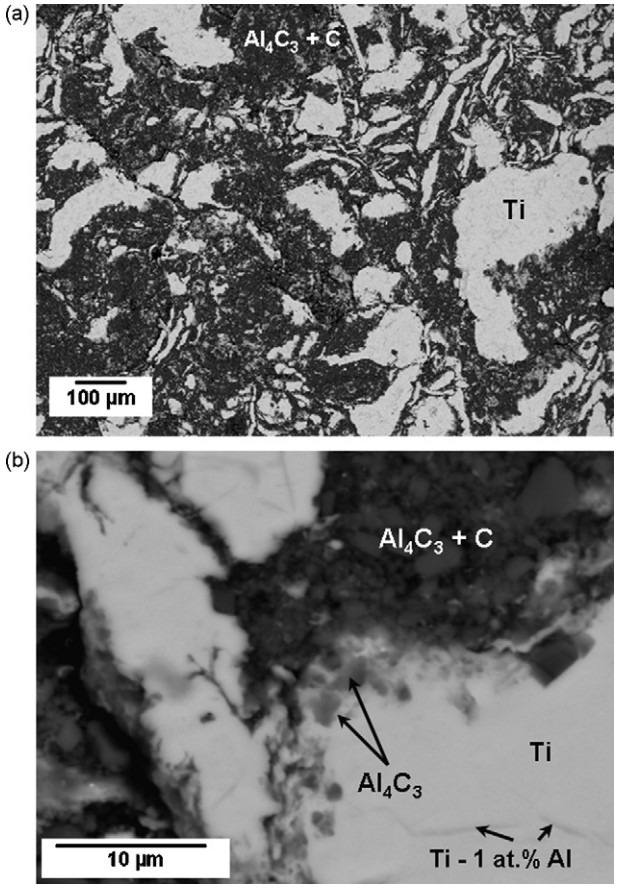

Fig. 5. Back-scattered SEM micrographs of the sample sintered at 570 °C for 1 h. (a) Overview of the sample and (b) closer view of the Ti particles embedded in the (Al_4C_3 + C) matrix.

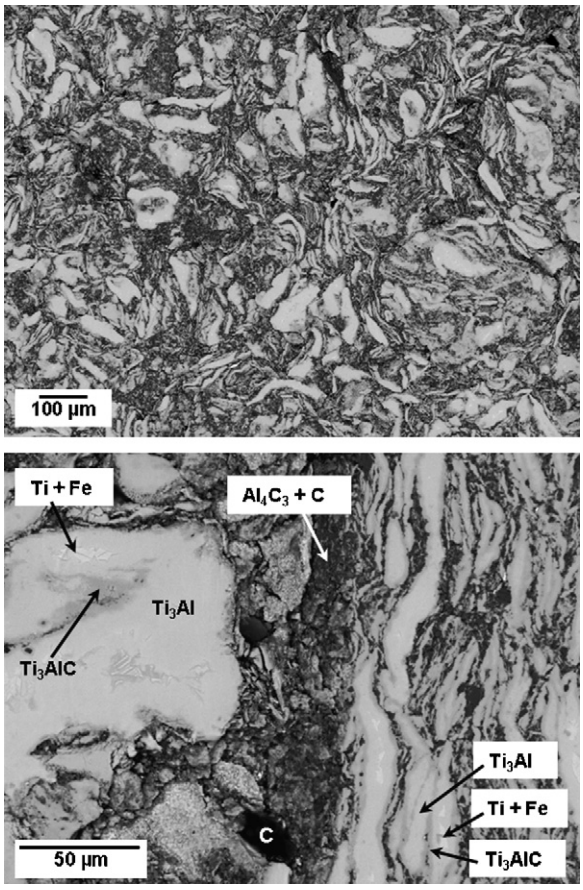

Fig. 6. Back-scattered SEM micrographs of the sample sintered at 800 °C for 1 h. (a) General view of the sample and (b) closer view of the microstructure of the different initial and intermediate phases.

set towards higher lattice spacing in the Ti_3Al structure may be attributed to the insertion of C atoms into Ti_3Al, and the formation of the resulting $Ti_3Al(C_x)$ solid solution. Ti_2AlC formation starts at about 1000 °C. The Ti_2AlC content increases from 1000 to 1400 °C whereas the content of Ti_3AlC and Ti_3Al phases decreases. More precisely, at 1200 °C, Ti_3AlC phase is no more detected while Ti_3Al content still decreases up to 1400 °C where it is reduced to zero. After sintering at 1300 and 1400 °C, Ti_3AlC_2 formation starts but the predominant phases are TiC and Ti_2AlC. Finally, it is important to mention that the TiC amount remains approximately constant in the temperature range 800–1400 °C.

To have a better understanding of the reaction paths leading to the Ti_2AlC formation, back-scattered SEM observations and corresponding EDS analyses were performed to localize the intermediate and final phases formed during sintering at different temperatures in the range 570–1400 °C.

A typical back-scattered SEM cross-section of the sample sintered at 570 °C for 1 h is displayed in Fig. 5. The microstructure appears to be the same as the one obtained after the milling process. Indeed, the sample consists in bright unreacted micrometric Ti particles embedded in a dark matrix composed of Al_4C_3 and C particles. Furthermore, on can observe some micrometric dark Al_4C_3 particles embedded in the close surface area of the Ti particles. Such an observation, that was already made after the milling process, can simply be attributed to the incorporation of these hard particles into the softer Ti ones during the milling process. A more detailed observation revealed the presence of darker areas in the Ti particles which correspond to local Al enrichment as confirmed by EDS analyses. Even if the use of this result obtained with this last technique should be taken with care, a concentration in Al into Ti close to 1 at.% was systematically obtained in these areas. This result tends to prove that Al diffusion into Ti, along preferential diffusion path such as grain boundaries or cracks, occurred during the sintering process. The insertion of Al into Ti defaults is confirmed by the XRD pattern obtained at 570 °C (see Fig. 3), which reveals the presence of a shoulder at higher lattice spacing for (0 0 2) and (1 0 1)Ti diffraction peaks.

As observed in Fig. 6, after sintering at 800 °C, smaller bright micrometric particles are uniformly distributed into the (Al_4C_3 + C) matrix. These bright particles are composed of a Ti core surrounded by Ti_3Al and $Ti_3Al(C_x)$ continuous layers; the $Ti_3Al(C_x)$ layer being in contact with the surrounding (Al_4C_3 + C) matrix. Some white Fe-rich areas, resulting from the contamination by the stainless steel container and balls used during the mechanical activation process, are detected inside the Ti core. Such a presence of Fe is detected in the whole temperature range investigated in this study. It is important to note that most of the bright particles observed at 800 °C are much smaller

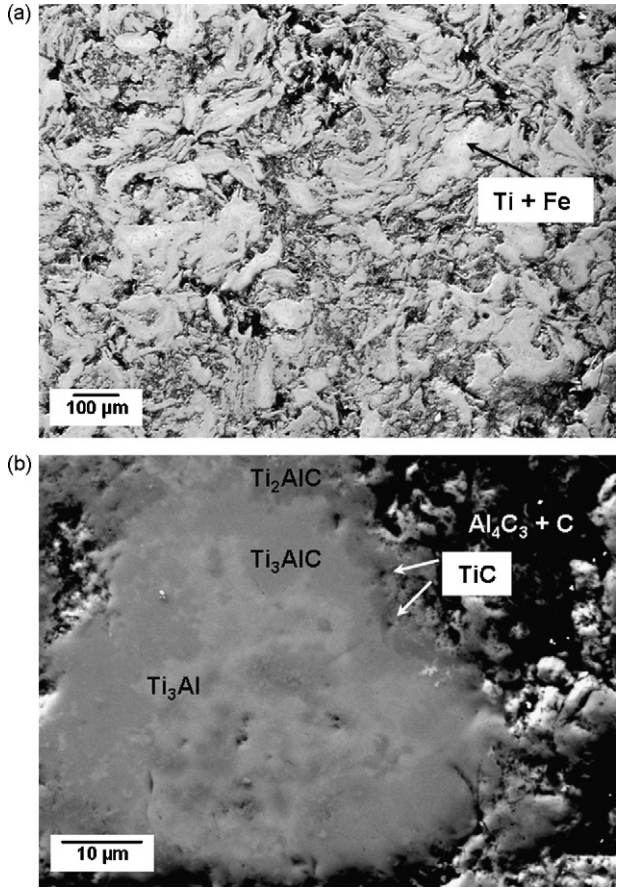

Fig. 7. Back-scattered SEM micrographs of the sample sintered at 1000 °C for 1 h. (a) Overview of the sample and (b) closer view of the microstructure of the different initial, intermediate and final phases.

that the Ti particles examined at 570 °C. It is well-known that atomic diffusion is favoured along defects and grain boundaries. Indeed, in the temperature range 570–800 °C, Al and C atoms diffuse more rapidly along these preferential diffusion paths to form Ti_3Al and Ti_3AlC. As a consequence, Ti particles observed at 570 °C are subdivided into smaller particles at 800 °C. Finally, some TiC particles are detected in the (Al_4C_3 + C) matrix.

After sintering at 1000 °C, Fig. 7 shows that most of the Ti particles have completely reacted with the (Al_4C_3 + C) matrix. At such a temperature, the particles embedded in the remaining (Al_4C_3 + C) matrix are constituted of a Ti_3Al core (light grey), and successive Ti_3AlC (grey) and Ti_2AlC (dark grey) layers from the core to the periphery of the particle. The external Ti_2AlC layer in contact with the (Al_4C_3 + C) matrix contains some black TiC particles.

Fig. 8 demonstrates that the sample sintered at 1300 °C is denser. The dense areas of this sample are mainly composed of sintered Ti_2AlC particles. Some black TiC particles and some white Fe-rich regions are also observed in dense areas. The porous parts surrounding the sintered Ti_2AlC areas consist of TiC particles. A brighter layer corresponding to the Ti_3AlC_2 phase is located at the periphery of the sintered Ti_2AlC areas, in contact with the porous regions made of TiC particles.

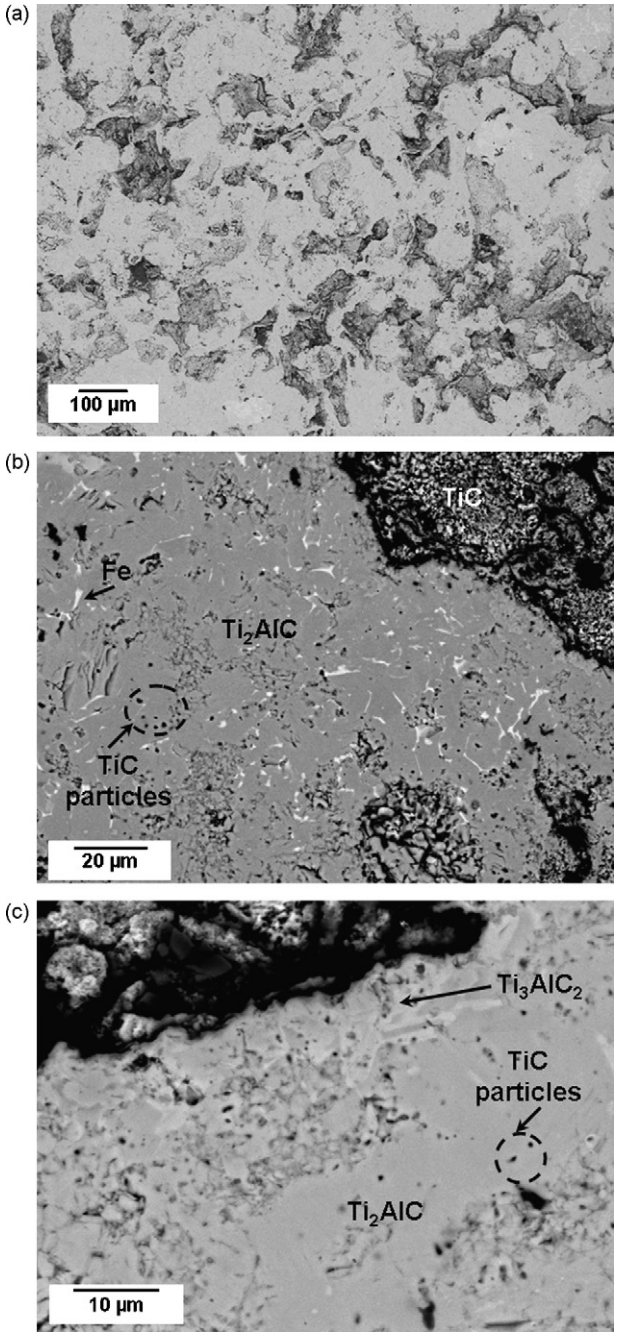

Fig. 8. Back-scattered SEM micrographs of the sample sintered at 1300 °C for 1 h. (a) General view of the sample, (b) closer view of the microstructure of the final phases, and (c) closer view of the Ti_3AlC_2 phase formed at the periphery of the sintered Ti_2AlC grains.

After sintering at 1400 °C, one can observe in Fig. 9 a uniform Ti_2AlC matrix containing some TiC black particles.

4. Discussion

Significant changes occur during high-temperature exposure as a result of Ti, Al_4C_3 and C interdiffusion. Based on XRD analyses and SEM observations, a possible reaction sequence responsible for the formation of Ti_2AlC from Ti/C/Al_4C_3 reactants is proposed:

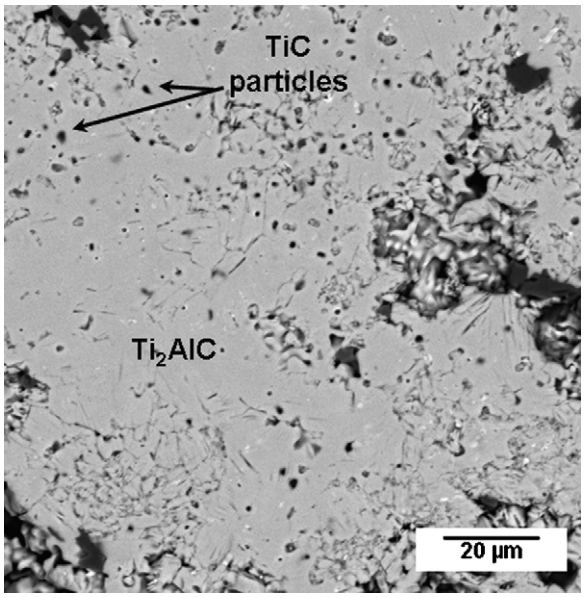

Fig. 9. Back-scattered SEM micrograph of the sample sintered at 1400 °C for 1 h.

In the range 570–1000 °C, XRD analyses demonstrate that the amount of initial reactant phases drastically decreases to reach zero at 1100 °C. Moreover, SEM observations show the existence of bright particles constituted of a Ti core surrounded by Ti_3Al and $Ti_3Al(C_x)$ continuous layers after sintering at 800 °C; the $Ti_3Al(C_x)$ layer being in contact with the surrounding (Al_4C_3 + C) matrix containing some TiC particles. Thus, reaction (i) can explain the formation of Ti_3Al and $Ti_3Al(C_x)$ intermediate phases, either at the interface between Ti particles and (Al_4C_3 + C) matrix or inside the defaults (principally at grain boundaries) of mechanically activated Ti particles (see Fig. 6).

$$(12+y)\mathrm{Ti} + \mathrm{Al_4C_3} \rightarrow 4[\mathrm{Ti_3Al(C_x)}] + y\mathrm{TiC_{3-4x/y}} \quad \text{(i)}$$

In the temperature range 800–900 °C, the formation of the Ti_3AlC phase at the interface between Ti_3Al and the surrounding (Al_4C_3 + C) matrix likely results:

- first, from dissolution of C atoms into Ti_3Al as revealed by the presence of an offset of the (2 0 1)Ti_3Al diffraction peak towards higher lattice spacing which may be attributed to the formation of the intermediate $Ti_3Al(C_x)$ solid solution.
- second, from precipitation of Ti_3AlC as the C solubility limit into $Ti_3Al(C_x)$ solid solution is reached.

Such a mechanism can be described by reaction (ii):

$$(1-x)\mathrm{C} + \mathrm{Ti_3Al(C_x)} \rightarrow \mathrm{Ti_3AlC} \quad \text{(ii)}$$

Reaction (i) can also explain the formation of sub-stoichiometric titanium carbide in the temperature range 570–800 °C concomitantly to Ti_3Al and $Ti_3Al(C_x)$ formation. This carbide formation can also result from reaction (iii) involving Ti and C reactants:

$$\mathrm{Ti} + x'\mathrm{C} \rightarrow \mathrm{TiC_{x'}} \quad \text{(iii)}$$

It is important to note that, in the ternary Ti–Al_4C_3–C system, $TiC_{x'}$ formation starts at a lower temperature than in the binary Ti–C system.[14] At 800 °C, some $TiC_{x'}$ particles are observed in the (Al_4C_3 + C) matrix. $TiC_{x'}$ formation proceeds at higher temperatures, as long as Ti/C interfaces exist. For temperatures higher than 1000 °C, TiC becomes stoichiometric as shown in Fig. 3.

At 1000 °C, Ti_2AlC formation can result from the reactions (iv) and (v) since Ti_2AlC phase is located at the interface between the Ti_3AlC layer and the (Al_4C_3 + C) matrix as observed in Fig. 7. Moreover, the Ti_2AlC layer observed after 1 h sintering at 1000 °C contains some TiC_x particles which can be involved in the formation of the Ti_2AlC phase.

$$8\mathrm{Ti_3AlC} + \mathrm{Al_4C_3} + \mathrm{C} \rightarrow 12\mathrm{Ti_2AlC} \quad \text{(iv)}$$

$$(8x'-1)\mathrm{Ti_3AlC} + x'\mathrm{Al_4C_3} + \mathrm{TiC_{x'}} \rightarrow (12x'-1)\mathrm{Ti_2AlC} \quad \text{(v)}$$

$TiC_{x'}$ content remains constant in the temperature range 800–1400 °C, which means that $TiC_{x'}$ formation still proceeds according to reaction (iii) to approximately provide the $TiC_{x'}$ amount consumed in reaction (v).

The Ti_2AlC content increases from 1000 to 1400 °C. For temperatures higher than 1000 °C, Ti and Al_4C_3 are no more detected according to the XRD detection limit. Thus, for these temperatures, reactions (iv) and (v) cannot explain Ti_2AlC formation. In the temperature range 1000–1200 °C, Ti_2AlC formation is accompanied, as demonstrated by XRD results, by the decline of the two intermediate Ti_3Al and Ti_3AlC phases. Thus, one can propose that these two phases are implied in the Ti_2AlC formation. At this stage, Ti_2AlC formation can result from reaction (vi) or (vii):

$$\mathrm{Ti_3AlC} + \mathrm{Ti_3Al} + 3\mathrm{C} \rightarrow 2\mathrm{Ti_2AlC} + 2\mathrm{TiC} \quad \text{(vi)}$$

$$\mathrm{Ti_3AlC} + \mathrm{C} \rightarrow \mathrm{Ti_2AlC} + \mathrm{TiC} \quad \text{(vii)}$$

Some small TiC particles are observed into Ti_2AlC particles; such an observation is compatible with these two reactions. Nevertheless, a reaction between Ti_3AlC and Ti_3Al would imply that Ti_2AlC is formed at the Ti_3Al/Ti_3AlC interface which is not the case in our SEM observations (see Fig. 7); Ti_2AlC is formed at the interface between Ti_3AlC and surrounding C. As a consequence, Ti_2AlC formation likely results from reaction (vii).

Nevertheless, XRD analyses demonstrate that the Ti_2AlC content increases up to 1400 °C while Ti_3AlC phase disappears at 1200 °C; Ti_3Al being detected up to 1400 °C. As Ti_2AlC is also formed at temperatures higher than 1200 °C, Ti_3AlC and Ti_2AlC phase formation kinetics must be very different. Indeed, on can assume that as soon as Ti_3AlC is formed according to the slow reaction (ii), it reacts to form Ti_2AlC according to the fast reaction (vii). Thus, one can explain that, Ti_3Al being present to form Ti_3AlC and the latter reacting so fast to form Ti_2AlC, Ti_2AlC can be formed from reaction (vii) with no trace of Ti_3AlC in the intermediate phases.

Finally, Ti_2AlC and TiC partially react, at 1300 and 1400 °C, to form small amount of Ti_3AlC_2 according to reaction (viii):

$$\mathrm{Ti_2AlC} + \mathrm{TiC} \rightarrow \mathrm{Ti_3AlC_2} \quad \text{(viii)}$$

To end this discussion part, it is important to compare our reaction mechanism for the formation of Ti_2AlC with those already proposed in the literature for the same system. Few studies of the reaction mechanisms responsible for the Ti_2AlC formation have been performed. Indeed, Khoptiar and Gotman[12] and Liu et al.[13] are, as far as we know, the only researchers, to have investigated Ti_2AlC reaction mechanisms starting with Ti, Al and C powder blends, using *a far from equilibrium synthesis method* called combustion synthesis (see description of the mechanism in the introduction part). Other studies related to Ti_3AlC_2 synthesis using reactive sintering[15] or pulse discharge sintering[16] reveals the reaction mechanisms operating during the formation of the intermediate Ti_2AlC phase.

The reactive sintering of $Ti/Al_4C_3/C$ mixtures at $1417° \pm 5\,°C$ to form the ternary carbide Ti_3AlC_2 has been studied in situ by neutron powder diffraction by Wu and Kisi.[15] These authors have demonstrated that a series of intermediate phases occur during the synthesis process beginning with the formation of β-Ti, TiC_x and Ti_3AlC in the temperature range 800–1400 °C. The formation of a further intermediate phase, Ti_2AlC, mostly occurred at 1417 °C. Starting with Ti, Al_4C_3, and C reactants, Wu and Kisi do not detect the presence of any Ti_3Al phase; moreover, Ti_2AlC formation mostly occurred at 1417 °C, a temperature higher than the one measured in the present study (1000 °C). Such a difference may be related to the mechanical activation of the reactants during the milling step. Indeed, mechanical activation increases the contact surface area between $Ti/Al_4C_3/C$ reactants, the diffusion paths are then reduced and the reactivity is increased.

It is suggested in[15] that Ti_2AlC formation could result from a number of reactions, such as:

$$8Ti + Al_4C_3 + C \rightarrow 4Ti_2AlC \quad (a)$$

$$8Ti_3AlC + Al_4C_3 + C \rightarrow 12Ti_2AlC \quad (b)$$

$$(8x-1)Ti_3AlC + xAl_4C_3 + TiC_x \rightarrow (12x-1)Ti_2AlC \quad (c)$$

As it was accompanied by the decline of Ti_3AlC and TiC_x phases, the most likely reaction path for the formation of Ti_2AlC has been attributed, by Wu and Kisi, to reaction (c). This reaction corresponds to reaction (v) of the present study, one of the two reactions used to justify the Ti_2AlC formation around 1000 °C. Note that the second reaction proposed in our study, i.e. reaction (iv), corresponds to the reaction (b) mentioned by Wu and Kisi.

Synthesis reactions of Ti_3AlC_2 through pulse discharge sintering starting with $Ti/Al_4C_3/TiC$ powder mixture has been investigated by Zou et al.[16] From XRD analyses, the intermediate phases formed at 800, 900, and 1100 °C are respectively Ti_3Al, Ti_3AlC, and Ti_2AlC according to Zou et al. Starting with $Ti/Al_4C_3/C$ powder blends in the present study, Ti_3Al and Ti_3AlC formation start at 800 °C, whereas Ti_2AlC is detected from 1000 °C. It appears that the nature of the reactants does not influence the formation temperature of these compounds since they are formed at about the same temperatures in the present paper.

On the basis of XRD analyses, Zou et al. have shown that the reactions during Ti_2AlC formation can be expressed as follows:

$$2Ti_3AlC + Al_4C_3 + 7Ti \rightarrow 5Ti_2AlC + Ti_3Al$$

$$7Ti_3Al + 2Al_4C_3 + 9TiC \rightarrow 15Ti_2AlC$$

These reactions demonstrate that the reaction path responsible for Ti_2AlC formation strongly depends on the nature of the reactants as the mechanisms proposed in[16] do not correspond to the one suggested in the present study.

5. Conclusion

In the temperature range 570–1400 °C, a series of intermediate phases has been observed ex situ during reactive sintering of Ti_2AlC from $Ti/Al_4C_3/C$ powder mixtures. The intermediate phases TiC_x, Ti_3Al, and Ti_3AlC start to form between 570 and 800 °C while the Ti and Al_4C_3 reactant phases are no more detected at 1100 °C. From XRD analyses, a set of four reactions appears as possible Ti_2AlC formation mechanisms. Nevertheless, intermediate phases content variations give strong evidence that Ti_2AlC formation mainly results from a reaction mechanism involving Ti_3AlC, Ti_3Al and C (reaction vi) or Ti_3AlC and C (reaction vii). From SEM observations, the increase of the Ti_2AlC content, in the temperature range 1100–1400 °C, results from the fast reaction between Ti_3AlC and remaining C; Ti_3AlC being formed from a slow reaction based on the dissolution of C atoms into the Ti_3Al phase. After sintering at 1400 °C for 1 h, the main phases present are Ti_2AlC and TiC.

Acknowledgment

The authors acknowledge Mr. Fabien Pontini for his technical help.

References

1. Jeitschko, W., Nowotny, H. and Benesovsky, F., Kohlen-Stoffhaltige Ternare Verbindungen H-phase. *Monatsh. Chem.*, 1963, **94**, 672.
2. Pietzka, M. A. and Schuster, J. C., Summary of constitutional data on the Al–C–Ti system. *J. Phase Equilib.*, 1994, **15**, 392.
3. Barsoum, M. W., Farber, L., Levin, I., Procopio, A., El-Raghy, T. and Berner, A., HRTEM of Ti_4AlN_3 or $Ti_3Al_2N_2$ revisited. *J. Am. Ceram. Soc.*, 1999, **82**, 2545–2547.
4. Barsoum, M. W. and El-Raghy, T., Synthesis and characterization of a remarkable ceramic: Ti_3SiC_2. *J. Am. Ceram. Soc.*, 1996, **79**(7), 1953–1956.
5. Barsoum, M. W., Brodkin, D. and El-Raghy, T., Layered machinable ceramics for high temperature applications. *Scripta Mater.*, 1997, **36**, 535–541.
6. Barsoum, M. W. and El-Raghy, T., Room temperature, ductile carbides. *Met. Mater. Trans.*, 1999, **30A**, 363–369.
7. Barsoum, M. W., The $M_{N+1}AX_N$ phases: a new class of solids thermodynamically stable nanolaminates. *Prog. Solid State Chem.*, 2000, **28**(1–4), 201.
8. Barsoum, M. W. and El-Raghy, T., A progress report on Ti_3SiC_2, Ti_3GeC_2, and the H-phases, M_2BX. *J. Mater. Syn. Process.*, 1997, **5**, 197–216.
9. Barsoum, M. W., Ali, M. and El-Raghy, T., Processing and characterization of Ti_2AlC, Ti_2AlN, and $Ti_2AlC_{0.5}N_{0.5}$. *Metall. Mater. Trans. A*, 2000, **31A**, 1857–1865.

10. Ivchenko, V. I., Lesnaya, M. I., Nemchenko, V. F. and Kosolapova, T. Y., *Porosh. Metall.*, 1976, **161**, 45.
11. Hong, X., Mei, B., Zhu, J. and Zhou, W., Study on the fabrication of Ti_2AlC by spark plasma sintering. *J. Chin. Ceram. Soc.*, 2003, **31**(10), 991–993.
12. Khoptiar, Y. and Gotman, I., Ti_2AlC ternary carbide synthesized by thermal explosion. *Mater. Lett.*, 2002, **57**, 72–76.
13. Liu, G., Chen, K., Zhou, H., Guo, J., Ren, K. and Ferreira, J. M. F., Layered growth of Ti_2AlC and Ti_3AlC_2 in combustion synthesis. *Mater. Lett.*, 2007, **61**, 779–784.
14. Dubois, S., Karnatak, N., Beaufort, M. F., Bourdarias, L., Renault, P. O. and Vrel, D., Influence of the mechanical activation on the TiC self-propagating high-temperature synthesis. *Mater. Technol.*, 2003, **18**(3), 158–162.
15. Wu, E. and Kisi, E. H., Synthesis of Ti_3AlC_2 from $Ti/Al_4C_3/C$ studied by in situ neutron diffraction. *J. Am. Ceram. Soc.*, 2006, **89**, 710–713.
16. Zou, Y., Sun, Z., Tada, S. and Hashimoto, H., Synthesis reactions for Ti_3AlC_2 through pulse discharge sintering Ti/Al_4C_3/TiC powder mixture. *Scripta Mater.*, 2006, **55**, 767–770.